Langmuir
Letter
pubs.acs.org/Langmuir

Doping-Induced Conductivity Transitions in Molecular Layers of Polyaniline: Detailed Structural Study

L. Cristofolini,*,† M. P. Fontana,† O. Konovalov,‡ T. Berzina,† and A. Smerieri†

†CNR-INFM-SOFT & Physics Department, University of Parma, Viale Usberti 7/A, Parma 43100, Italy, and ‡European Synchrotron Radiation Facility, ESRF, 6 rue J. Horowitz, Grenoble, France

Received July 17, 2009. Revised Manuscript Received September 17, 2009

We report detailed structural investigations, by synchrotron X-ray reflectivity (XRR), grazing incidence diffraction (GID), and space-resolved grazing incidence X-ray-induced fluorescence (GIXF), on the structure of molecular layers of polyaniline (PANI) that can be converted from insulating to conducting state simply by doping. We first address the simpler, but more intriguing, system, i.e., a floating monolayer of PANI on different subphases, for which we found a typical thickness of 28(1) Å, not much affected by the doping process. For the doped film we also found an internal lateral structure, with in-plane spacing of 3.5 Å—albeit with a small coherence of 3−4 repeat units only—compatible with face-to-face interchain stacking of phenyl rings, in agreement with the literature. By GIXF we could confirm the crucial role of Cl^- intercalation in the doping process of the PANI film: under doping conditions (0.1 M HCl subphase) the Cl^- intake is 8 times larger than in nondoping conditions (0.1 M KCl subphase). Multilayers transferred onto solid substrate were studied also as a function of the applied voltage, as this system constitutes the core of an electrochemically controlled device whose strongly nonlinear characteristic make it useful for applications to adaptive networks for complex information processing. By the application of an electrostatic field of 140 V/m, Cl ionic migration was observed confined to the polymeric film surface.

Introduction

Alkali cation intercalation is well-known to alter the structure and the electronic properties of many systems, including fullerenes, nanotubes, and organic conductors in general, often because of a combined effect of charge transfer and of induced structural modification. For instance, in fullerenes this gives rise to a variety of phases including those with metallic and insulating characters,[1,2] superconductivity,[3] and magnetic ordering.[4,5] Moreover, when Li ions are involved, peculiar diffusive behavior can be observed.[6,7] This is also the case of polyaniline (PANI)[8] which has a long history in the research of conducting polymers[9−13] and whose conductivity depends strongly on its doping level and redox state: the insulating emeraldine base form can be transformed into its conducting salt by doping, usually with hydrochloric acid. In particular, a recent report[14] clearly shows that if properly prepared, PANI bulk films do show proper metallic behavior, as evidenced by the temperature dependence of the resistivity. The metallic form of PANI can be transformed back to a nonconducting state by e.g. exposure to a base or also to an alkali salt. In particular, Li ions intercalation and deintercalation is well-known to modify PANI conductivity.[15] These doping transitions are reversible, and therefore conductivity of the PANI layer can be restored and controlled electrochemically by application of a reducing or oxidizing potential.

An electrochemically controlled three-electrode device consisting of a heterojunction between a PANI multilayer (the active component) and a thicker solid electrolyte (Li^+-doped poly(ethylene oxide) (PEO)) was extensively studied by some of us;[16−18] its strongly nonlinear characteristic was connected to the possibility of modulating the conductivity by varying the applied voltage to the PANI layer, through the combined effect of redox processes and doping−dedoping ionic fluxes from the solid electrolyte. This device had memory of its previous functioning, i.e., it was a functional memristor; this made it particularly interesting for applications to adaptive networks for complex information processing device. Thus, a thorough understanding of the mechanisms responsible for the conductivity modulation and memory effects is essential for these and other types of applications.

In this paper we present a study of the structural changes in the PANI layer due to the conductivity variations and doping−dedoping processes. The measurements were performed XRR and GID, which provide us with high-resolution structural information, and GIXF, which is a direct element specific, surface

*To whom correspondence should be addressed: Tel +39 0521 905276.

(1) Kroto, H. W., Fischer, J. E., Cox, E., Eds. *The Fullerenes*; Pergamon Press: Oxford, 1993.
(2) Prassides, K.; Keshvarz, M.; Hummelen, J. C.; Beer, E.; Bellavia, C.; Cristofolini, L.; Gonzalez, R.; Lappas, A.; Murata, Y.; Malecki, M.; Srdanov, V.; Wudl, F. *Science* **1996**, *271*, 1833.
(3) Holczer, K.; Klein, O.; Huang, S. M.; Kaner, R. B.; Fu, K. J.; Whetten, R. L.; Diederich, F. *Science* **1991**, *252*, 1154.
(4) Stephens, P. W.; Bortel, G.; Faigel, G.; Tezge, M.; Janossy, A.; Pekker, S.; Oszlanyi, G.; Forro, L. *Nature* **1994**, *370*, 636.
(5) L. Cristofolini, L.; Lappas, A.; Vavekis, K.; Prassides, K.; Derenzi, R.; Ricco, M.; Schenck, A.; Amato, A.; Gygax, F.; Kosaka, M.; Tanigaki, K. *J. Phys.: Condens. Matter* **1995**, *7*, L567.
(6) Cristofolini, L.; Facci, P.; Fontana, M. P.; Cicognani, G.; Dianoux, A. J. *Phys. Rev. B* **2000**, *61*, 3404.
(7) Riccò, M.; Belli, M.; Mazzani, M.; Pontiroli, D.; Quintavalle, D.; Janossy, A.; Csanyi, G. *Phys. Rev. Lett.* **2009**, *102*, 145901.
(8) Kang, E. T.; Neoh, K. G.; Tan, K. L. *Prog. Polym. Sci.* **1998**, *23*, 277–324.
(9) MacDiarmid, A. G. *Synth. Met.* **1997**, *84*, 27.
(10) MacDiarmid, A. G.; Chiang, J. C.; Richter, A. F.; Epstein, A. *J. Synth. Met.* **1987**, *18*, 285.
(11) Diaz, A. F.; Logan, J. A. *J. Electroanal. Chem.* **1980**, *111*, 111.
(12) Watanabe, A.; Mori, K.; Iwabuchi, A.; Iwasaki, Y.; Nakamura, Y.; Ito, O. *Macromolecules* **1989**, *22*, 3521.
(13) Focke, W. W.; Wnek, G. E.; Wei, Y. *J. Phys. Chem.* **1987**, *91*, 5813.
(14) Lee, K.; Cho, S.; Park, S. H.; Heeger, A. J.; Lee, C. W.; Lee, S. H. *Nature* **2006**, *441*, 65–68.
(15) Joo, J.; Song, H. G.; Jeong, C. K.; Baeck, J. S.; Lee, J. K.; Ryu, K. S. *Synth. Met.* **1999**, 98,215.
(16) Berzina, T.; Erokin, V.; Fontana, M. P. *J. Appl. Phys.* **2007**, *101*, 024501.
(17) Smerieri, A.; Erokin, V.; Fontana, M. P. *J. Appl. Phys.* **2008**, *103*, 094517.
(18) Cristofolini, L.; Fontana, M. P.; Berzina, T.; Camorani, P.; Nabok, A., *Phys. Rev. E*, submitted for publication.

sensitive, and nondestructive technique in which the fluorescence from the ions (chemical sensitivity) is recorded as a function of the grazing angle of incidence (depth sensitivity) to test for the presence of ions in the structure of the molecular layer and therefore directly measure the ionic depth distribution which could then be related to the electrical properties of the PANI layer.

We studied PANI layers in different doping conditions. We addressed the Langmuir layer at the air−water interface, and then Langmuir−Schaeffer (LS) multilayers deposited onto solid substrate, also connected with electrodes to probe the effect of the applied voltage on the ionic distribution.

The results presented here show unambiguously that the insulator−conductor conversion of PANI film is accompanied by Cl anion intercalation and specific structural changes. Our data also have relevance for the so-called metallic nature of the conducting form of PANI and in particular on the intriguing question of whether even a Langmuir monolayer at the air−water interface can be considered metallic, a question which has been much debated for both inorganic and organic films.[19−22]

In a recent paper we have shown, mainly by ellipsometric techniques, that indeed conductivity is retained by PANI even in the form of a Langmuir monolayer.[18] Here we present microscopic structural confirmation of those data.

Experimental Section

Poly(ethylene oxide) (PEO) (average M_w ca. 8 000 000), KCl, and CsCl were purchased from Sigma. Polyaniline emeraldine base (PANI) (average M_w ca. 100 000, catalogue no. 576379) was purchased from Aldrich. Polyaniline powder first was dissolved in 1-methyl-2-pyrrolidone (NMP) in the concentration of ∼1 mg/mL (mother solution). Then NMP with 10% of toluene was added to some amount of mother solution to obtain the final concentration of 0.1 mg/mL and filtered through Millipore filter (Omnipore PTFE, hydrophilic, pore diameter 0.2 μm). Toluene was added to facilitate solution spreading. This solution was used for the preparation of the Langmuir monolayer and Langmuir−Schaefer films. Pure water prepared with a Milli-Q system was used as the subphase (resistivity 18.2 MΩ cm, pH 7.0). The composition of the subphase was varied by adding HCl or KCl up to 0.1 M concentration or other salts as indicated in each experiment.

Langmuir isotherms were routinely obtained in a KSV 5000 trough or in our homemade trough both to check the monolayer quality for deposition and to prepare the monolayer at the air−water interface at the proper surface pressure for the measurements. Typical compression speed was 10 mm/min. After compression of the PANI monolayer up to the target surface pressure of 10 mN/m, a variable number of layers (from 1 to 60) were deposited by the horizontal lifting LS technique onto Si substrates or onto glass slides with evaporated chromium electrodes.

X-ray measurements were performed at the ID10B line of the ESRF synchrotron facility, at the incident energy $\varepsilon = 8.06$ keV. In reflectivity measurements at the air/water interface a theta/theta geometry was employed. Grazing incidence diffraction (GID) measurements were performed with an angle of incidence on the film of $\mu = 0.11°$, i.e., 75% of the critical angle for total reflection at the air/water interface, and collecting the diffracted intensity as a function of the scattered angle, after Soller slits collimation, by a linear position sensitive detector. The reflected-scattered intensity was analyzed both as a function of the in-plane Q_{xy} and of the out-of plane Q_z exchanged momentum.

Reflectivity data were subsequently analyzed with our own software, developed in the Matlab computing environment, which calculates the reflectivity curve for a given model according to the so-called "Parratt recursive approach".[23,24] In this case one calculates the transmission and reflection Fresnel coefficients at each interface. In order to reproduce the reflectivity curve of a real multilayer, a structured model of independent layers, each with uniform electron density, has to be provided. Roughness of real layers is accounted for using the Névot−Croce approximation,[25] which implies scaling of the reflectivity at the interface between layers a and b by a pseudo-Debye−Waller factor $\exp(-2k_ak_b\sigma^2)$, σ being the roughness rms value and k_ak_b representing the z-component of the wave vector for layers a and b, respectively. The quality of the fit is evaluated weighting the discrepancy between data and model either by the uncertainty of the data (true χ^2 test) or by a factor which is inversely proportional to the reflectivity itself. The latter strategy gives comparatively more weight to the high-Q data, which, albeit affected by larger uncertainty, contain more physical information.

Grazing incidence X-ray fluorescence (GIXF) was detected as a function of the incidence angle, from grazing incidence, across the critical angle and well above it to provide a reference to the bulk ionic concentration. For the data analysis we developed our own program code, following the guidelines of ref 26. We recall here that below the critical angle for total external reflection an evanescent wave propagates at the surface with an angle-dependent penetration depth $\xi = {}^1/_2\mathrm{Im}(k_z)$ where k_z is the normal component of the incident wave vector in the solution.[27] The penetration depth assumes a minimum value at grazing incidence ($\xi = 4.6$ nm for air/water interface) and increases with the angle to diverge at the critical angle. Beyond the critical angle, the penetration depth increases to micrometers, being limited only by the attenuation length, thus providing a reference for the overall detection system efficiency as a function of the ionic known bulk concentration. After energy calibration, the fluorescence of each element was extracted as a function of the incidence angle (or of the beam position when appropriate) and normalized to the elastic (Compton) scattered intensity, to account for many geometrical factors including the beam footprint and the detector limited angular acceptance.

Results

Langmuir Layers. In the top panel of Figure 1 we report the X-ray reflectivity curve measured on a PANI monolayer at the air−water interface as a function of the incidence angle, at the surface pressure of 10 mN/m. Data are normalized to the Fresnel reflectivity for the air/water interface. The film structure, shown in the inset of the same figure, was best modeled by two slabs: one close to the air surface, accounting for the main part of the film, for a thickness of 20(1) Å, with higher electron density (ρ = 0.41(1) $e^-/Å^3$), and one close to the water surface, with lower electron density (ρ = 0.37(1) $e^-/Å^3$) and thickness 8(1) Å. The roughness of each interface (σ = 3−3.5 Å) is comparable with that of pure water surface due to capillary waves. The reduction of electron density in the lower part of the film could be ascribed to water molecules interpenetrating the film structure. We also note that the total film thickness, which is 28(1) Å, is in agreement with our previous ellipsometric estimate obtained from deposited multilayers, 27(1) Å.[18] The fact that the film structure is best reproduced by a two-slab model, with lower electron density close to the water surface, is a clear indication that the PANI film close to the water surface hosts some amount of water molecules

(19) Mott, N. F. *Metal-Insulator Transitions*; Taylor & Francis: London, 1990.
(20) Phillips, P.; Dalidovich, D. *Science* **2003**, *302*, 243–247.
(21) MacDiarmid, A. G. *Curr. Appl. Phys.* **2001**, *1*, 269–279.
(22) Heeger, A. J. *Rev. Mod. Phys.* **2001**, *73*, 681–700.
(23) Parratt, L. G. *Phys. Rev.* **1954**, *95*, 359–369.
(24) Daillant, J.; Gibaud, A. *X-Ray and Neutron Reflectivity: Principles and Applications*; Springer: Berlin, 1999.
(25) Névot, L.; Croce, P. *Rev. Phys. Appl.* **1980**, *15*, 761–779.
(26) Padmanabhan, V.; Daillant, J.; Belloni, L.; Mora, S.; Alba, M.; Konovalov, O. *Phys. Rev. Lett.* **2007**, *99*, 086105.
(27) Born, M.; Wolf, E. *Principles of Optics*, 7th ed.; Cambridge University Press: Cambridge, 1999.

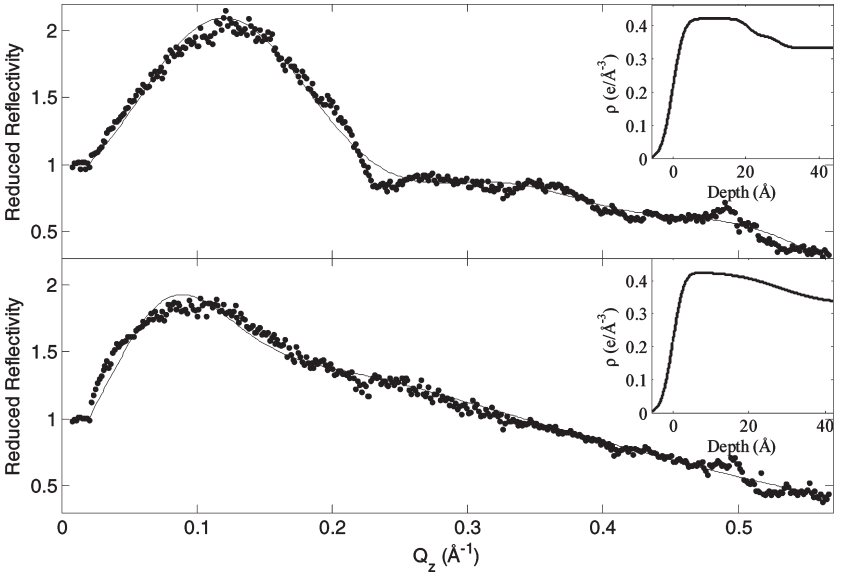

Figure 1. Top: XRR (data and best fit) of a Langmuir film of insulating PANI on water at the surface pressure of 10 mN/m, scaled by the Fresnel reflectivity, vs the vertical momentum Q_z (best fit model in the inset). Bottom: same for conducting PANI (i.e., on 0.1 M HCl subphase).

intercalating within the polymeric chains, suggesting a sparse configuration with some of the chain ends immersed in water.

In the bottom panel of Figure 1 we report the reflectivity for a conducting PANI film at the same value of surface pressure 10 mN/m, on the acidic subphase given by a solution 0.1 M HCl. The data are again scaled by the Fresnel reflectivity for the bare air/water interface; the continuous line is the best fit obtained with the model represented in the inset, comprising of a single slab with thickness of 28(1) Å, with slightly higher electron density (ρ = 0.43(1) $e^-/Å^3$) and a larger value of the roughness of film/water interface (σ = 5−8 Å). From the comparison of the two structures we can draw two consequences: first, the overall film thickness does not show any appreciable variation upon the doping process. In second place, we can integrate the electron density along z to obtain the surface electron density, which is 11.10 $e^-/Å^2$ for the insulating film and increases to 12.04 $e^-/Å^2$ for the conducting one. This increase can be related to the partial inclusion of the Cl^- ions within the film. Its small size could be due to the increase of roughness that could smear and make less apparent the variation of electron density.

We then conclude that while insulating emeraldine base PANI on pure water forms a loose structure with branches protruding into the subphase, its corresponding conducting salt forms a more homogeneous structure, with no evident ramifications into the subphase, which is best modeled by a single slab of higher electron density and roughness, compatible with the inclusion of Cl ions within the film.

We also performed GID measurements: at the surface pressures relevant to our study (10 mN/m) the GID pattern is characterized by the presence of characteristic "rod" peaks, a signature of true 2D molecular order, with no trace of Debye rings, which on the contrary would be the signature of 3D polycrystalline arrangement. In fact, Debye rings do show up at the highest pressures studied, namely 26 mN/m, where true collapse occurs, thus confirming that we are able to discriminate between a well-ordered 2D film and the collapse into 3D crystallites at the interface.

In the bottom panel of Figure 2 we report the X-ray GID intensity measured on the same PANI monolayer at the air−water interface at impinging angle 75% of the critical angle. From the map presented, clear vertical rods can be identified with the in-plane position Q_{xy} = 1.0 and 1.8 $Å^{-1}$. We emphasize here that the observed diffracted intensity arises from true 2D diffraction, being constituted by Bragg vertical rods only. On the contrary, from highly compressed and therefore collapsed films, we observed 3D Debye rings, which in turn are the signature of 3D diffraction, arising from the collapsed structure of the film.

In the top panel of the same Figure 2 we report the GID intensity integrated in the vertical direction up to Q_z = 0.4 $Å^{-1}$ as a function of the in-plane momentum Q_{xy} after appropriate background subtraction. The two curves correspond to the PANI film on pure water (circles) and on 0.1 M HCl subphase. PANI in the former film is known to be insulating; the latter is expected to have metallic character, as confirmed by our independent ellipsometric measurements. Note, in the metallic phase on HCl, the presence of two diffraction peaks at 1.0 and 1.8 $Å^{-1}$ with a prominent shoulder at 1.45 $Å^{-1}$ currently under investigation (a peak at this position has been reported in ref 14) which are not present in the insulating phase on pure water. In particular, most of the intensity is concentrated in the highest Q peak which corresponds to a spacing of 3.5 Å, which matches the face-to-face interchain stacking distance between phenyl rings. This suggests a strongly planar chain conformation with reduced torsion angles between the phenyl ring and the plane of the backbone, resulting in elongation of the effective conjugation length.[14] However, from the relatively large breath of the peak we can also evaluate the lateral coherence length being only of the order of a few (3−4) repeat units. These results are entirely consistent with our FT-IR and Raman data published in ref 16.

Two possible reasons could explain the lack of diffraction peaks from insulating PANI: either structural inhomogeneity or the lack of the electronic contrast which is provided by the presence of chlorine atoms in doped PANI. It seems quite reasonable that the complex formed by the H^+ bound to the amine group, and the relevant Cl^- counterion, follow and "decorate" the naturally weak periodicity of the PANI Langmuir layer, making enough contrast for the GID pattern to be observed only from the conductive layer.

As anticipated, we also measured the X-ray fluorescence spectra from Langmuir monolayers at different surface pressure

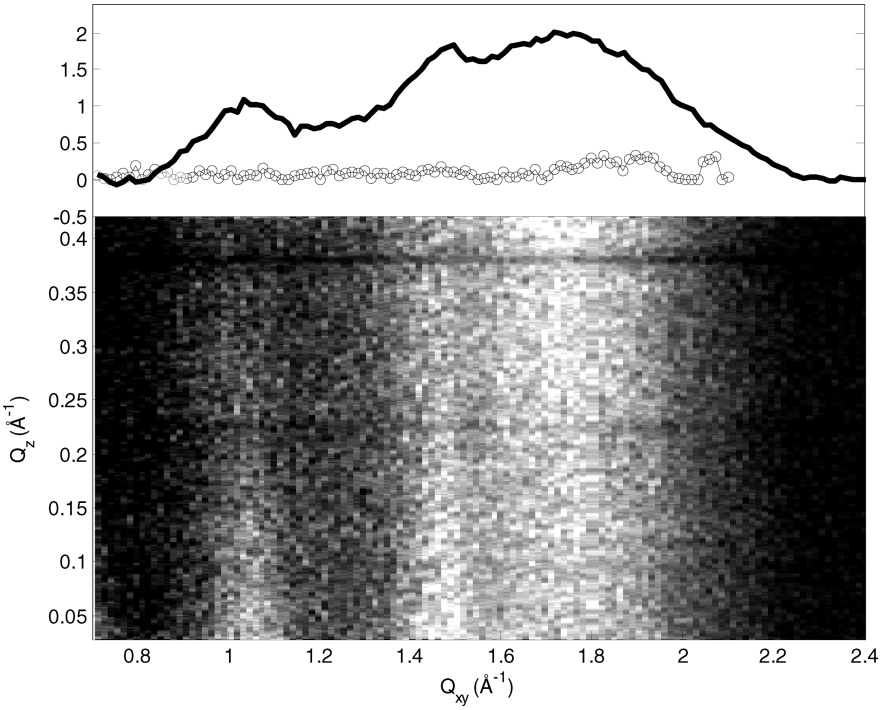

Figure 2. Top panel: GID intensity for insulating (circles) and conducting (line) Langmuir films of PANI at 10 mN/m. Note the presence of coherence peaks in the conducting phase, which are not present in the insulating phase. Bottom panel: corresponding GID pattern for the conducting film. Note the presence of vertical rods, indicating 2D coherence, in the region around 1.0 and 1.8 Å^{-1}.

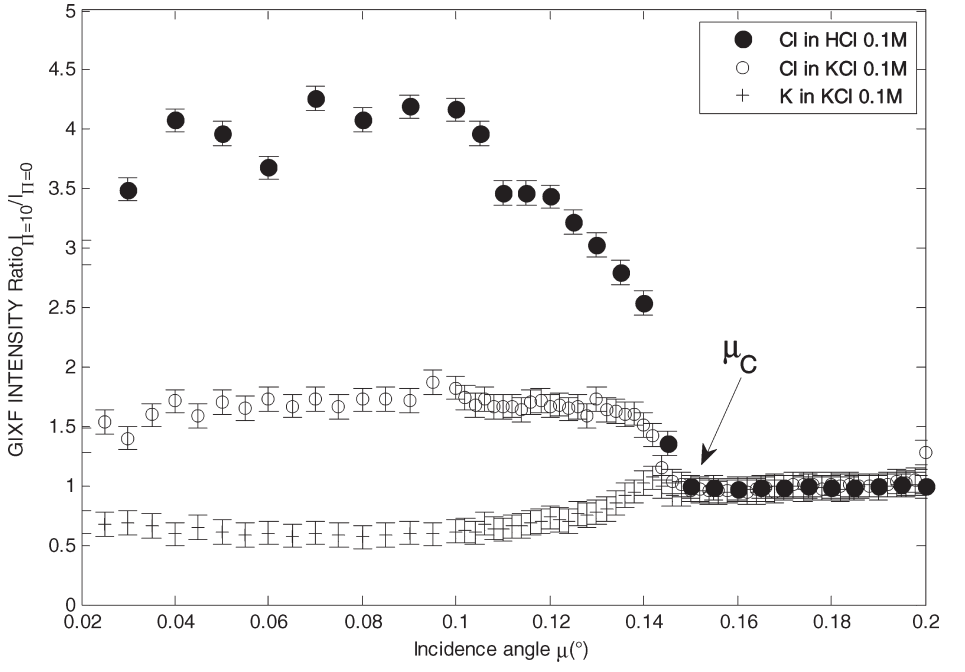

Figure 3. GIXF intensity for Cl and K, as a function of the incidence angle, from Langmuir layer of PANI on different subphases: HCl 0.1 M and KCl 0.1 M, after normalization to GIXF intensity on the same subphase in the absence of a Langmuir layer. The arrow marks the critical angle position.

on different subphase (pure water, HCl 0.1 M, and a mixture of HCl 0.1 M and KCl 0.1M) as a function of the incidence angle below and above the critical angle. Data were analyzed in energy, and Gaussian peaks were fitted in correspondence of the fluorescent emission of K, Cl, and Ar species (the latter originates from the atmosphere surrounding the sample, thus providing an internal consistency check) besides analyzing the quasielastic (Compton) scattering used for data normalization.

In Figure 3 we report the amplitude of the peak corresponding to the Cl fluorescence intensity from a PANI monolayer on different subphases: HCl 0.1 M and KCl 0.1 M after calibration from the fluorescence intensity measured from the bulk, i.e., with the incoming X-ray beam incident above the critical angle. Each intensity is also normalized to that measured in the same conditions but *in the absence* of any film, thus accounting for the extra intensity due to ions inglobated in the film or located close to the

surface. The first result apparent from the figure is a general increase in the Cl signal in both cases. The Cl intake is however 8 times larger in the presence of HCl, i.e., under doping conditions. Two consequences might be drawn from this result. First, Cl anions are weakly attracted by the PANI monolayer, and at the same time the K^+ cations are repelled in the same fashion. This is in agreement with the known cationic nature of the PANI monolayer in this conditions. The second, more important result is that the doping process is not merely H^+ attachment to the film but also intercalation of the H^+Cl^- complex within the PANI molecular layer structure. In other words, doping proceeds via the incorporation of Cl anions within the layer.

PANI Films Deposited on Solid Substrate. Deposited multilayers of PANI proved to be too rough to provide any usable reflectivity curve, in agreement with their roughness, measured by AFM to lie in the range of 10 nm, for the best samples. Investigation is in progress on how to produce smoother deposited samples. Nevertheless, we were able to investigate the fluorescence signal arising from these samples and analyze it as a function of the beam position. Thus, we investigated the effects of exposing a PANI film, made of 48 LS monolayers, to HCl and NH_3 vapors. The sample was originally one of our devices doped with KCl, so we expected to detect chlorine and potassium even before the exposure to the vapors. Also in this case we recorded fluorescence as a function of the incidence angle below and above the critical angle, data were analyzed in energy, and peaks were fitted in correspondence of the fluorescent emission of K, Cl, Cs, and Ar besides analyzing the quasielastic (Compton) scattering used for data normalization. Different positions along the sample were recorded, with and without an applied voltage, so as to detect any change in the ion distribution.

As a first check, we followed the PANI film doping by HCl vapors. For this reason we performed a lateral scan in 0.5 mm steps over the whole predoped film while measuring the Cl fluorescence intensity to check the film overall homogeneity. The signal was found to be constant within 5%. We repeated the measurement after exposure to fresh HCl vapors, and the Cl fluorescence intensity increased by 25%, as expected also on the grounds of our results from Langmuir layers. Finally, we repeated the scan after exposure to ammonia vapors, which are known to convert the conducting emeraldine salt to the insulating emeraldine base form, and the Cl fluorescence intensity dropped to a value about 15% of its original intensity, signifying expulsion of Cl anions in correspondence to the dedoping process. Incidentally, we note that potassium and argon intensities did not change after the doping and dedoping processes. We also monitored the conductivity variations due to the doping and dedoping reactions: the pristine film had $R > 200$ MΩ (resistivity $\rho > 1$ kΩ cm), which dropped after the doping to $R = 16$ kΩ ($\rho = 0.08$ Ω cm) and returned to the pristine value after exposure to the ammonia vapors.

We also applied *in real time* an electric field in the direction parallel to the film surface and normal to the incoming X-ray beam and observed the effects of an applied voltage on the distribution of ions as detected by their fluorescence intensity. For this experiment we used LS film of HCl-doped PANI with thickness 168 nm. At one end of the sample we placed an electrical contact using eutectic paste; at the other end, at the distance of 14 mm, we placed a silver wire immersed in CsCl-doped poly(ethylene oxide) (PEO). We selected to work with Cs salt because of its high-energy fluorescent emission. However, a drawback of this choice was that Cs possesses intrinsically a lower ionic mobility.

We measured fluorescence at two values of the incidence angle, one below and one above the critical angle, in order to discriminate between the behavior of the ions at the surface of the film and in the bulk. We performed three runs of measurements: the first with no voltage between the electrodes, the second applying a −1 V bias to the eutectic paste electrode, and the third applying a −2 V bias to the same electrode while keeping the other electrode grounded. In the graphs that follow, the negatively biased electrode is at $x = -7$ mm, while the electrode at ground potential is at $x = +7$ mm.

Data intensities were corrected to account for the attenuator of the X-ray beam, and are normalized to Compton scattering, to account for geometrical effects due to the nonideal conformation of our sample. In particular, we collected fluorescence from Cl with the excitation beam impinging below (at 0.2°) and above (at 0.5°) the critical angle for total reflection from the polymeric film (see the Supporting Information). In the first case we are probing the topmost layer, of the order of 5 nm, while in the second case we probe the bulk of the film.

We found that when the bias reached −2 V (for an average electric field of 143 V/m), a significant migration of Cl^- ions occurred away from the negative electrode which diffuse within the surface of PANI film, as probed with an incidence angle below critical angle. At the same time the bulk of PANI film is not interested by the Cl migration, as detected by the data collected above critical angle (see the corresponding figures in the Supporting Information). Notably, no Cs migration could be detected, possibly because of its much larger ionic radius, as its fluorescence signal is constant thorough the various scans. As a consistency check we also recorded the Ar fluorescence intensity and the Compton scattering, which do not vary at all in the course of our measurements, thus ruling out the possibility that sample movement and/or misalignment would be responsible for the variation of intensity of Cl fluorescence. Therefore, the fact that preferential ion migration occurs in the topmost part of the film is presumably related to the presence of a "pseudo liquid" layer at the polymer/air interface, which exhibits enhanced molecular mobility, with respect to the bulk of the polymer at the same temperature, as detected by a number of techniques, including second harmonic generation (SHG) and ellipsometry.[28,29] Data analysis is in progress; however, we anticipate that this is related to the mechanism controlling the conductivity of PANI films.[17]

We also note that the kinetics of the doping/dedoping process, which is of particular relevance for the correct functioning of the electrochemical device, has been studied in the past by us by monitoring the time-dependent V/I characteristics.[17] Several technical difficulties discouraged us from repeating this study using synchrotron radiation X-rays. However, the results we report here should encourage such an effort.

Conclusions

In conclusion, by synchrotron X-ray reflectivity, grazing incidence diffraction, and depth-resolved X-ray-induced fluorescence, we clarified the structure of molecular layers of polyaniline (PANI) that can be converted from insulating to conducting state simply by doping. We first address the experimentally difficult but simpler system represented by a floating monolayer of PANI on different subphases. In this case we could measure the film thickness (28(1) Å for both insulating and conducting PANI) in total agreement with our previous ellipsometric estimate. We also found that, while a reasonably defined molecular layer is formed by both the insulating and the conducting forms (taking into

(28) Jerome, B.; Commandeur, J. *Nature* **1997**, *386*, 589.
(29) Cristofolini, L.; Arisi, S.; Fontana, M. P. *Phys. Rev. Lett.* **2000**, 85 4912.

account the polymeric nature of the film), nevertheless we encountered some important differences: insulating PANI is best modeled assuming two layers: a compact layer on top and a water intercalated layer below, suggesting a sparse configuration with some of the chain ends immersed in water; on the contrary, conducting PANI forms a more homogeneous structure, which is best modeled by a single slab of high electron density, with however quite a large overall roughness.

By GID we could identify broad coherence peaks from the conducting phase of PANI, in agreement with the literature[14] and corresponding to a spacing of 3.5 Å with a lateral coherence of the order of a few (3−4) repeat units, which matches the face-to-face interchain stacking distance between phenyl rings, implying a strongly planar chain conformation. By GIXF on a Langmuir layer we could identify the process of doping with the intercalation of H^+Cl^- complexes within the PANI molecular layer.

By X-ray fluorescence we could follow the chemical doping/dedoping cycle on a deposited multilayer, confirming the results obtained from the Langmuir layer about the crucial role of Cl^- intercalation/deintercalation. We finally studied a multilayer subject to an applied voltage, in which field-induced ionic migration was clearly identified, localized in the topmost part of the molecular layer, often referred to as the "liquid layer".[30,31]

This preliminary data should encourage extension of our study to the full three-electrode electrochemically controlled device as it is functioning. This would be particularly interesting for this functional memristor,[32] in view of its possible applications to advanced and innovative information processing.

Acknowledgment. We acknowledge the financial support of the Future and Emerging Technologies (FET) programme within the Seventh Framework Programme for Research of the European Commission, under the FET-Open grant agreement BION, number 213219. We also acknowledge Y. Gunaza for help with the experiments and for the preparation of the artwork for the TOC graphic.

Supporting Information Available: Fit of the reflectivity curves through the Parratt algorithm, with error bars of the fits. Evidence for the Cl ion migration under voltage applied as detected by space resolved GIXF, with X-ray incidence above and below the critical angle for total reflection.

This material is available free of charge via the Internet at http://pubs.acs.org/.

(30) Qi, D.; Fakhraai, Z.; Forrest, J. A. *Phys. Rev. Lett.* **2008**, *101*, 096101.
(31) Fakhraai, Z.; Forrest, J. A. *Science* **2008**, *319*, 600.
(32) Strukov, D. B.; Snider, G. S.; Stewart, D. R.; Williams, R. S. *Nature* **2008**, *453*, 80.